Journal of Power Sources 214 (2012) 40–50

Contents lists available at SciVerse ScienceDirect

Journal of Power Sources

journal homepage: www.elsevier.com/locate/jpowsour

A linear time-invariant model for solid-phase diffusion in physics-based lithium ion cell models

Xiao Hu [a,*], Scott Stanton [a], Long Cai [b], Ralph E. White [b]

[a] ANSYS Inc., Canonsburg, PA 15317, USA
[b] Department of Chemical Engineering, University of South Carolina, Columbia, SC 29208, USA

HIGHLIGHTS

- An LTI model, in the form of a state space model, is proposed for solid-phase diffusion in physics-based lithium ion cell models.
- The proposed model can be used for spherical and non-spherical particles.
- Impact of different particle shapes on electrochemical performances can be investigated.
- The model is much faster than solving the full model.

ARTICLE INFO

Article history:
Received 1 March 2012
Received in revised form
16 April 2012
Accepted 18 April 2012
Available online 25 April 2012

Keywords:
Lithium ion battery
Linear time-invariant modeling
Vector fitting
Solid-phase diffusion

ABSTRACT

Physics-based lithium ion models are widely used to predict the electrochemical behavior of lithium ion cells. The implementation of such a model typically requires solving a diffusion problem in solid particles. A linear time-invariant (LTI) model is proposed for the solid-phase diffusion problem. This LTI model can be used for spherical and non-spherical particles. For spherical particles, results from using the LTI model are compared with those from solving full diffusion equation, and excellent agreement is achieved. The LTI model solves only a few equations, and thus it runs much faster than the model solving the full diffusion equation. Impact of particle shapes on the electrochemical behavior is investigated after the model is validated.

1. Introduction

The lithium ion battery is a preferred candidate as a power source for hybrid electric vehicle (HEV) and electric vehicle (EV) due to its outstanding characteristics such as high energy density, high voltage, low self-discharge rate, and good stability among others. Physics-based lithium ion models are widely used to predict the electrochemical behavior of lithium ion cells [1–3]. The implementation of such a model typically requires solving a diffusion problem in solid particles, which are used to model the porous electrodes. Due to the large number of particles involved, the particle shapes are assumed to be spherical so that the diffusion equation becomes one dimensional. However, it is still computationally expensive to solve a large number of 1d diffusion equations. For particles of arbitrary shapes or more general porous structures, three dimensional diffusion equations are required to characterize the diffusion process in such structures. A physics-based model, which involves solving 3d diffusion equations, becomes prohibitively expensive computationally.

For spherical particles, several methods have been proposed to reduce the size of the problem. They belong to either the *global* approach or the *local* approach. In the *global* approach, the entire model is reduced. Such a *global* approach is used in [4] through proper orthogonal decomposition (POD). In such an approach, the space of the solution is estimated by testing system responses from *typical* boundary conditions to a full model. A set of basis are then formed for the solution space in such a way that the leading coordinates have much larger magnitude and thus the rest of the coordinates can be truncated. The reduced model is then formulated based on the new truncated basis. Because the physics-based model is highly non-linear, when actual boundary conditions differ from the *typical* boundary conditions used to identify the reduced model the error could be large. This approach cannot be

* Corresponding author. Tel.: +1 734 213 1261; fax: +1 734 213 0147.
E-mail address: xiao.hu@ansys.com (X. Hu).

0378-7753/$ – see front matter © 2012 Elsevier B.V. All rights reserved.
doi:10.1016/j.jpowsour.2012.04.040

extended to non-spherical particles easily since a full model is needed in the first place before a reduced model could be generated. Another *global* approach is proposed in [5]. In this approach, a full model is linearized and transfer functions are created for the linearized model. Errors could be large in using such an approach if perturbation is large since linearization assumes small perturbation. The method also relies on spherical particles for an analytical transfer function and thus cannot be extended to non-spherical particles.

Another popular approach is the *local* approach, in which only the linear diffusion equation is reduced and the non-linear part of the model is intact. Different *local* methods differ in how to obtain approximate solutions to the diffusion problem for a spherical particle. Approximation can be performed either in the time-domain or in the frequency-domain. One time-domain approach is to take advantage of superposition [1,2]. Another time-domain approach makes the assumption that the concentration within each spherical particle can be approximated with a parabolic profile [6,7]. A relatively recent time-domain approach is to obtain an approximate solution by truncating the analytical solution of an infinite series and then adding an estimate term for the truncation error [8]. In all of the time-domain *local* methods mentioned, spherical particles are assumed. In frequency-domain *local* approximation methods, a state space model is created to approximate the transfer function of the system. In Ref. [9], high-order poles of the transfer function are truncated and the lower-order poles are grouped together and approximated using a state space model. In Ref. [10], a discrete-time state space model is derived from a known transfer function. In Refs. [9,10], analytical transfer functions are assumed to be known, and thus both methods are limited to spherical particles.

In this paper, an LTI model, a frequency-domain *local* approach, is proposed to accurately model the diffusion process for spherical and non-spherical particles. This method shares similarity with [9] and [10] in that it also seeks a state space model that approximates the transfer function of the system. However, the current method does not assume a known transfer function. The transfer function is calculated numerically and thus it can be applied to non-spherical particles. The way to identify the state space model is also different. The method used in Ref. [9] does not give the same accuracy as the LTI method in this paper. Compared with Ref. [10], the current approach obtains the continuous-time state space model directly rather than having to obtain the discrete-time state space model first. The LTI method has been widely used to model devices and subsystems for the purpose of transient analysis in power systems [11,12], signal integrity characterization of microwave systems [13,14], and battery thermal systems [15,16]. In applying the LTI method, one essentially obtains the transfer function of the system *numerically* (or by testing in some cases) and then a state space model is identified to have the same transfer function using the vector fitting method [17]. Afterward, the state space model can be used to simulate the system in the time-domain. The LTI approach can give highly accurate results and yet the size of the model can be very small if the state space model is properly identified. Note that the LTI approach also relies on linearity, but it does not require the existence of an analytical solution since the transfer function of the system is obtained *numerically* (or by testing). For the current application, this implies that the method can be used for particles of any shape.

The paper is organized as follows. Section 2 describes the LTI approach for the solid-phase diffusion problem in particles. Section 3 integrates the LTI model into the physics-based model using spherical particles and validates its results against a full model solving particle diffusion equations directly. In Section 4, non-spherical particles are used and the impact of different shapes of particles on the electrochemical behavior is investigated. Finally, Section 5 is the conclusion.

2. LTI modeling for particle solid-phase diffusion

In using the LTI approach, the problem is treated like a system. A system is an entity that processes a set of input signals (or simply called inputs) and yields another set of output signals (or simply called outputs). In such a system view, only the input/output relationship of the system is of interest to the user and the inner structure of the system is not. In the solid-phase diffusion problem, the molar flux at the particle surface as a function of time is used as the input and the surface-averaged concentration increase at the particle surface as a function of time is used as the output. We are interested in the relationship between the surface molar flux and averaged surface concentration increase. Concentration distribution inside a particle is not of great interest. Solid-phase diffusion problem so described is a system. More importantly, it is not only *a* system, but it is also an LTI system. Any state space model is also an LTI system. One important feature about LTI systems is that if two LTI systems have the same impulse or step response, the two systems behave identically in that the outputs of the two systems are the same provided that the inputs to the two systems are the same. This feature allows us to use the state space model to simulate the solid-phase diffusion problem provided that its step response is curve-fitted to that of the solid-phase diffusion problem. Note that if two LTI systems have the same impulse or step response, they have the same transfer function. So, when matching the step response of two LTI systems, effectively we are matching the transfer function of the two LTI systems. Since the size of the state space model is small, it runs very fast compared with the full model which solves the complete diffusion equation directly using numerical methods.

The diffusion of lithium ions in a solid-phase particle follows the Fick's law and is described by the following partial differential equations:

$$\frac{\partial c}{\partial t} = D\nabla^2 c \tag{1}$$

$$c(\vec{x}, 0) = c_0 \tag{2}$$

$$-D\frac{\partial c}{\partial \vec{n}}\bigg|_{\Omega} = j(t) \tag{3}$$

where c is the concentration of lithium in the solid particle; c_0 is the initial concentration of lithium in the solid particle, assumed to be a constant; D is the solid-phase diffusion coefficient for lithium in the particle, assumed to be constant; $j(t)$ is the boundary molar flux, assumed to be a function of time only for each particle; and Ω denotes the boundary of the particle, which is assumed to fixed. We are interested in the relationship between $j(t)$ and averaged surface concentration increase of the system. Since the diffusion equation and the boundary condition are linear and diffusivity is a constant, the system so described is an LTI system.

A general state space model is typically written as follows:

$$\begin{aligned} \dot{x} &= Ax + Bu \\ y &= Cx + Du \end{aligned} \tag{4}$$

x is the state vector; y is the output vector; u is the input vector; A, B, C, D are constant coefficient matrices of proper sizes. Since Eqn. (4) is linear with constant coefficients, the system is an LTI system. For the state space model used to simulate the solid-phase diffusion

problem, x has no physical meaning; y is a scalar representing averaged surface concentration increase; u is a scalar representing the transient flux $j(t)$. A critical step in LTI modeling is to identify matrices A, B, C, D such that the state space model gives the same step response as the original diffusion problem governed by Eqn. (1)–(3). Once that is accomplished, characteristics of LTI systems guarantee that the state space model can be used to replace Eqn. (1)–(3) to model the relationship between the surface molar flux and averaged surface concentration increase with excellent accuracy.

To demonstrate the LTI approach, state space models are constructed for three different solid-phase structures, a spherical particle, an elliptical particle, and a more general porous structure. In the first example, a spherical particle is used. The first step in LTI model identification is to obtain the step response of the system modeled. In order to obtain the step response of the particle diffusion problem, the diffusion problem is solved numerically using FLUENT, a CFD code from ANSYS. The concentration distribution at the end of the step response simulation is shown in Fig. 1 along with the geometry and mesh used in the CFD model. Note that any CFD code can be used to solve the particle diffusion problem by using analogy between thermal diffusion and species diffusion.

After the diffusion problem is solved for its step response, a state space model of Eqn. (4) is identified by curve-fitting its step response to that of the CFD model. The curve-fitting was performed in the frequency-domain using the vector fitting (VF) method [17]. A brief introduction of the VF method applied to the diffusion problem is provided in Appendix A. The curve-fitting results are shown in Fig. 2. It can be seen that the state space model gives the same step response as the CFD model solving Eqn. (1)–(3). The excellent accuracy in Fig. 2 indicates that the curve-fitting by the VF method is very accurate for this diffusion problem. The state space model has an order of 7, and so only 7 ordinary differential equations are solved in the state space model. Higher order state space models can be used for greater accuracy. But from Fig. 2, it shows that an order of 7 is sufficient, and validation in Section 3 also indicates that 7th order is accurate enough when such a model is integrated into physics-based lithium-ion cell models. After the state space model is identified, it can be used to simulate the diffusion problem under *any* transient flux boundary rather than just step flux boundary.

For a spherical particle, its step response can be obtained analytically [8]. So, the state space model could also be identified using the analytical solution. Such fitting results and its corresponding state space model are provided in Appendix B for reference.

Note that the model generation process of the LTI approach does not depend on the shape of the particles. In the second example, an elliptical particle is used. The model generation process is the same

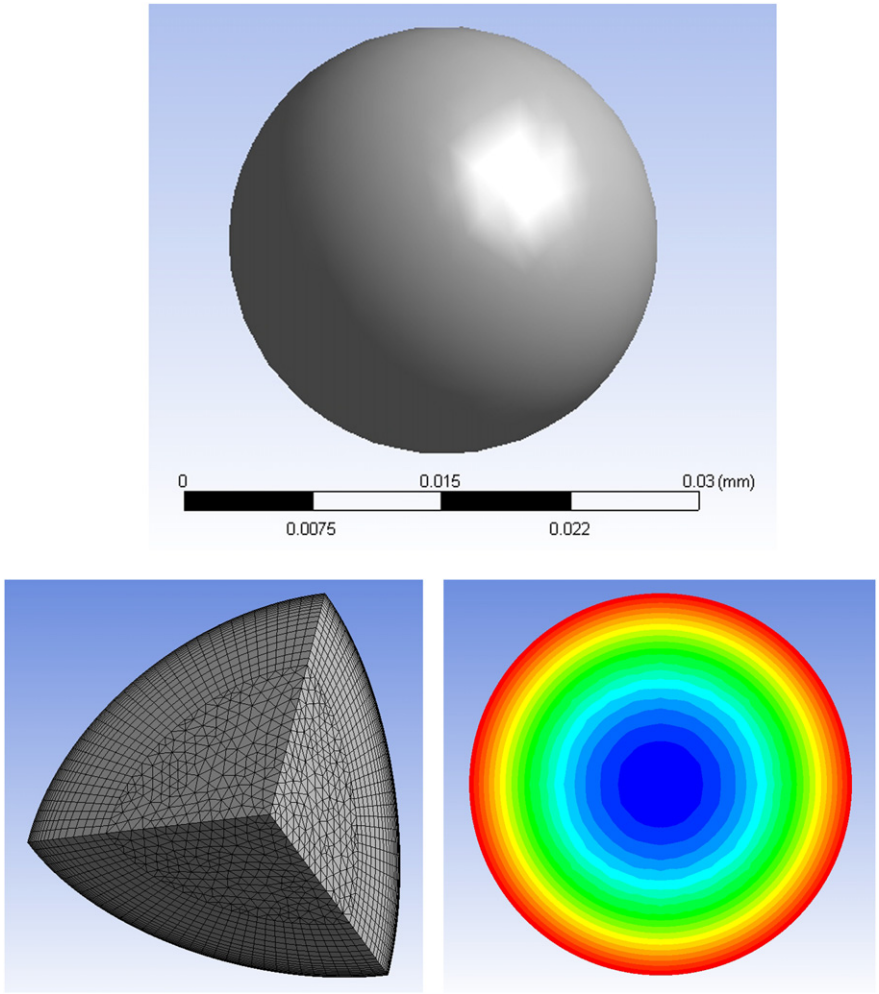

Fig. 1. Geometry and mesh for a spherical particle and its concentration distribution at the end of a step response run.

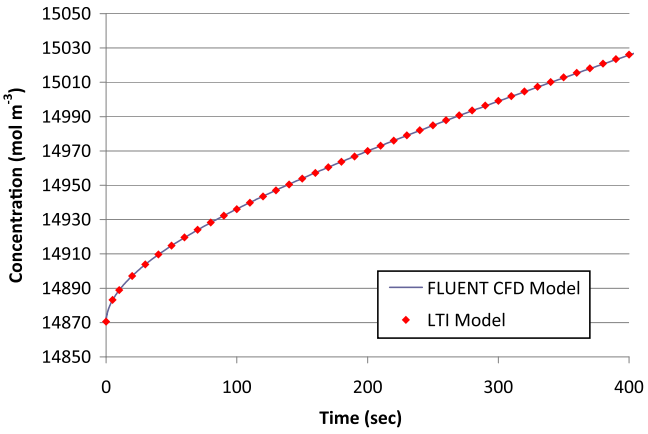

Fig. 2. Step responses from the CFD model and the LTI model for the spherical particle.

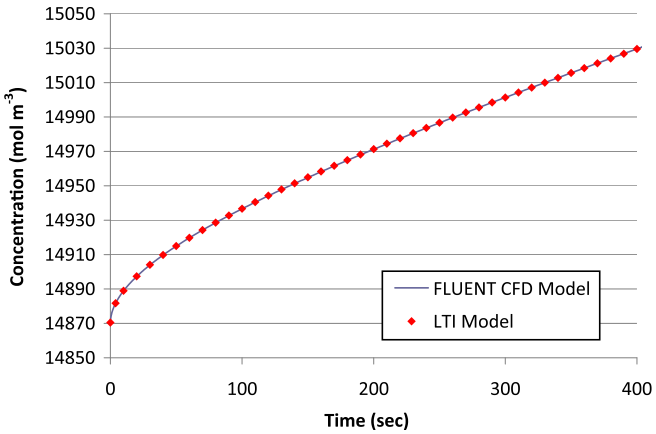

Fig. 4. Step responses from the CFD model and the LTI model for the elliptical particle.

as before. The concentration distribution at the end of the step response simulation along with the geometry and mesh used in the CFD model is shown in Fig. 3. Step responses from the CFD model and the LTI model are compared in Fig. 4. The excellent agreement shown in Fig. 4 indicates that curve-fitting performed by the VF method is excellent. This also implies that subsequent simulation by the LTI model under *any* transient flux $j(t)$ will give excellent accuracy.

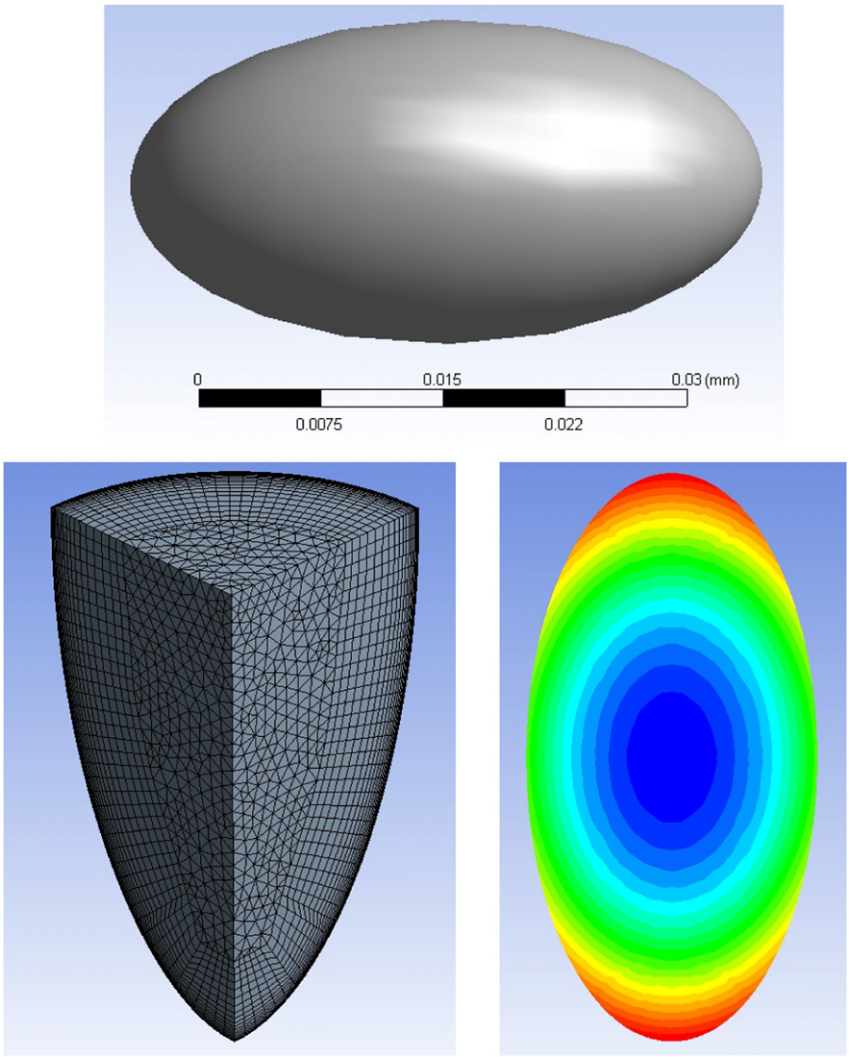

Fig. 3. Geometry and mesh for an elliptical particle and its concentration distribution at the end of a step response run.

The above elliptical example showed that the model generation process of the LTI approach is quite general. As a matter of fact, the porous structure of electrodes does not even have to be modeled using particles. Instead, any porous structure shape could be used without simplification. In this third example, a porous structure is used, which consists of spherical particles packed together with overlapping. For simplicity, this porous structure will be referred to as a *porous particle* in the rest of the paper. For this porous particle, the LTI model identification process is the same as before. The concentration distribution at the end of the step response simulation along with the geometry and mesh used in the CFD model is shown in Fig. 5. Step responses from the CFD model and the LTI model are compared in Fig. 6. Since concentration changes rapidly close to time of zero, a plot using log time scale is also shown in Fig. 6. Both plots in Fig. 6 showed excellent accuracy. High accuracy near time of zero is important for accurate prediction of transient behavior of a battery cell as shown shortly. Log time scale plots for the spherical and elliptical particles are also excellent. For simplicity, only the log time scale plot for the porous particle is shown.

The claim, that an LTI model could be used to simulate the diffusion problem under *any* transient flux of $j(t)$ provided that its step response matches well with that of the CFD model, is verified next. To do that, a rather arbitrary flux of $j(t)$ shown in Fig. 7 is used as the input to the CFD model and the corresponding LTI model for

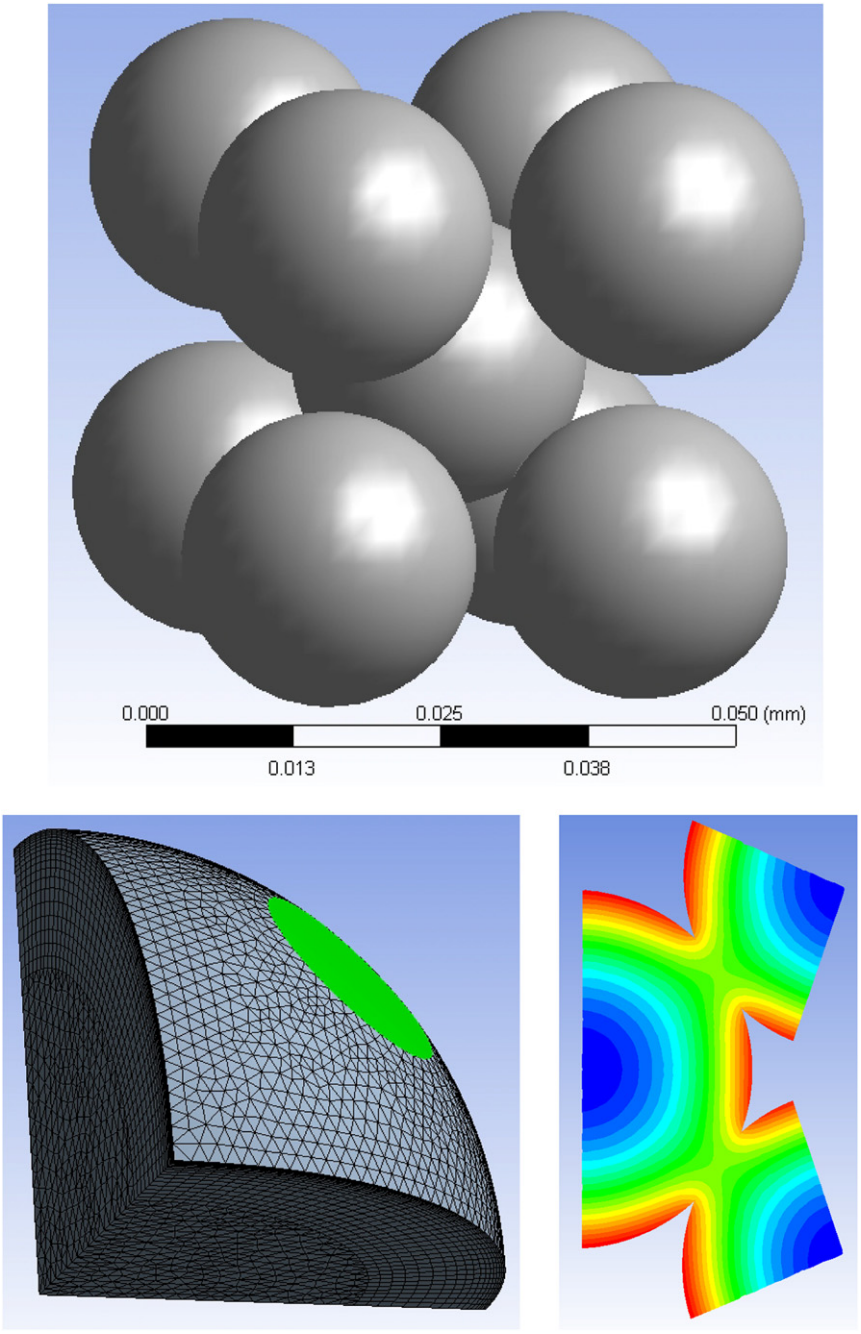

Fig. 5. Geometry and mesh for a porous particle and its concentration distribution at the end of a step response run. The green patch on the mesh denotes the overlapping region. (For interpretation of the references to color in this figure legend, the reader is referred to the web version of this article.)

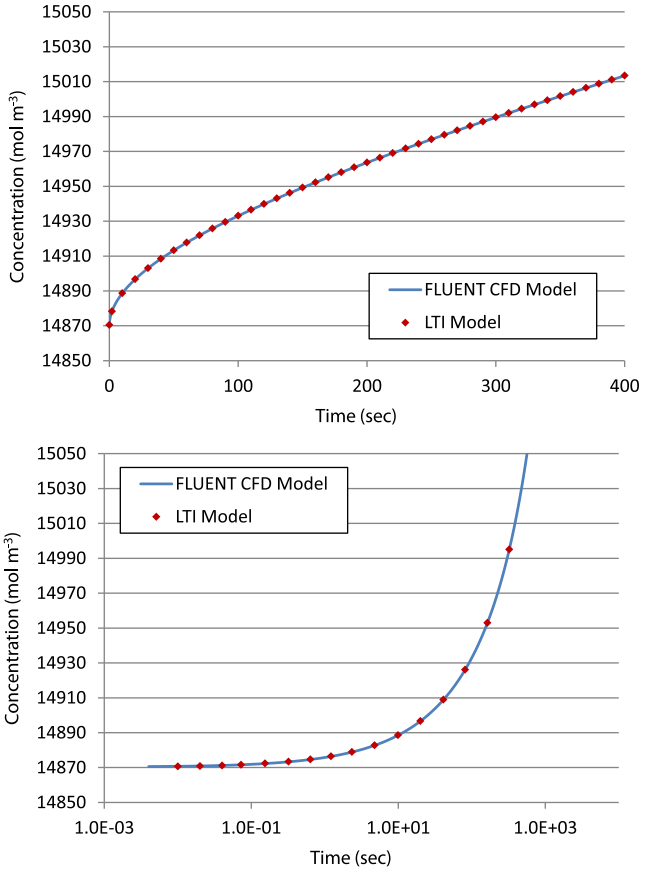

Fig. 6. Step responses from the CFD model and the LTI model for the porous particle. a) Regular scale on time. b) Log scale on time.

the porous particle. And their surface concentration results are then compared in Fig. 8. It is clear from Fig. 8 that the state space model gives excellent results under such an arbitrary transient flux of $j(t)$. Therefore, the claim is verified.

If a spherical particle and an elliptical particle are created to have the same volume, the difference in surface area would cause different surface concentration behavior. The elliptical particle has more surface area and therefore under the same surface flux its surface concentration increases more quickly. On the other hand, if the same total flux, namely the surface integration of $j(t)$, is applied

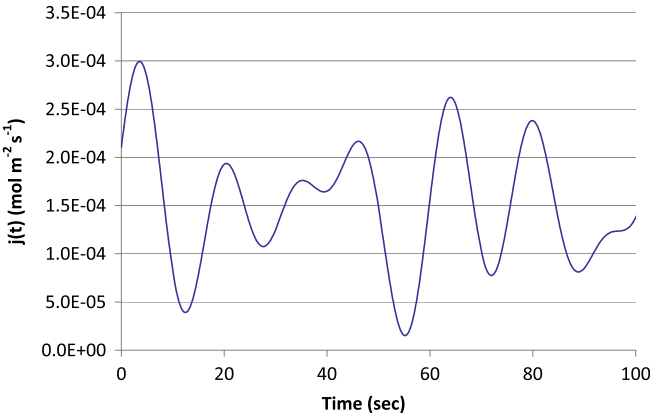

Fig. 7. An arbitrary boundary flux function $j(t)$ for testing.

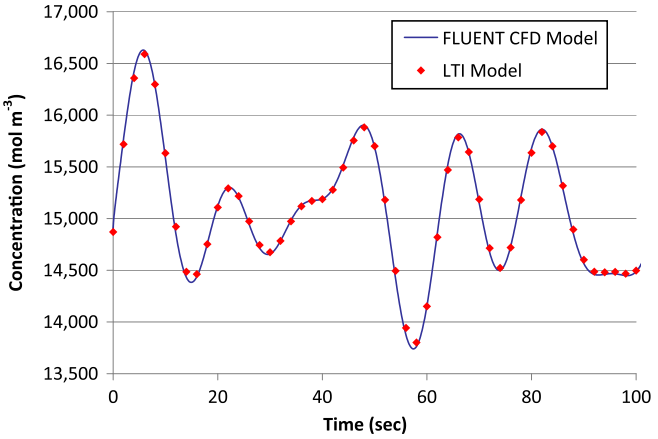

Fig. 8. Surface concentration from the CFD model and the LTI model under $j(t)$ shown in Fig. 7 for the porous particle.

to the two particles, the elliptical particle experiences smaller flux and thus its surface concentration increases less rapidly. The second scenario can be used to discuss the impact of different particle shapes on battery performance. The same argument above also applies to particles of different volumes and porous particles after proper scaling. The porous particle used in this paper, which is generated using spherical particles of the same size but with overlapping, has the opposite effect compared with the elliptical particle. This is because the porous particle has less surface area compared with the spherical particle per unit volume. Fig. 9 shows surface concentration of the three different particles under the same total flux, and the different behavior is what was just discussed. Larger surface area from the elliptical particle would make such a particle less prone to saturation and depletion. On the other hand, smaller surface area from the porous particle would make such a particle more prone to saturation and depletion. Impact of different particle shapes on battery performance is discussed in details in Section 4.

3. LTI model validation

In Section 2, LTI models are created and validated in isolated environments. In this section, the LTI model is validated when

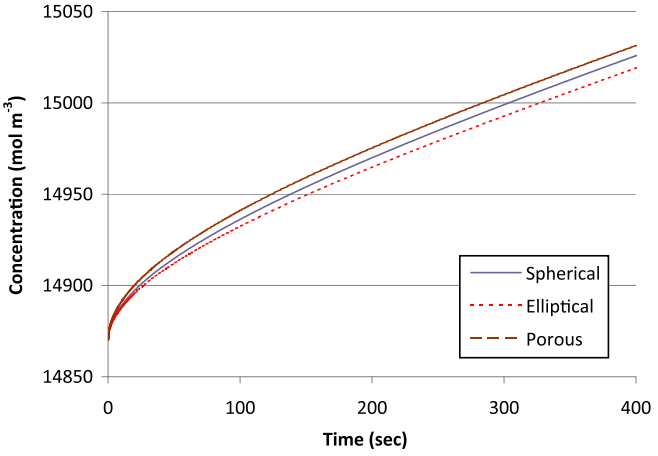

Fig. 9. Step responses of all three particles under the same total flux.

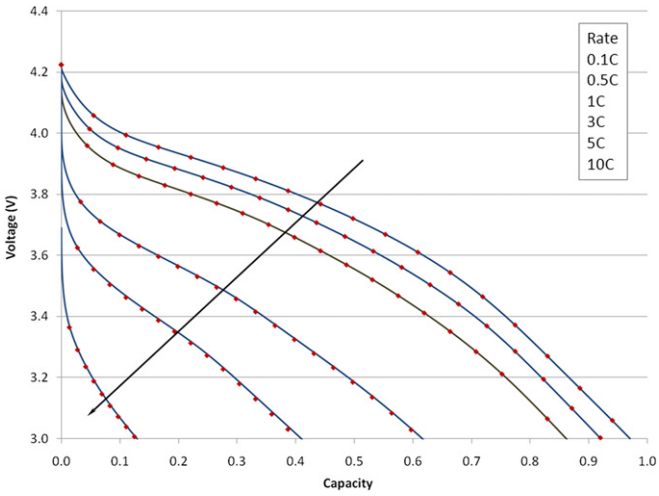

Fig. 10. Cell potential vs. capacity at different discharge rates using the full model (denoted by solid lines) and the reduced model (denoted by dotted lines).

integrated into the physics-based lithium ion cell model. Such a model will be referred to as the reduced model. For comparison, a model solving the complete solid-phase diffusion equation directly is created. This model will be referred to as the full model. Spherical particles are used since the full model can only allow for spherical particles. Properties and dimensions of the two models are otherwise identical and they are all from Ref. [4]. Both models are created using the VHDL-AMS modeling language and solved in Simplorer, a system simulator from ANSYS. Generation of physics-based lithium ion cell models using VHDL-AMS modeling language is discussed in detail in Ref. [18].

Fig. 10 showed the cell discharge curves using the full model and the reduced model. It can be seen from Fig. 10 that excellent results are obtained by using the reduced model even at a discharge rate of 10 C. For 10 C, the full model needs 200 equations for each particle to obtain accurate results when spatial discretization is uniform, and for the rest of the discharge curves, 100 equations per particle is used to obtain adequate accuracy using uniform spatial discretization. Fig. 11 showed the comparison of concentration at four specified interfaces. Again, excellent results are achieved by using the reduced model. Fig. 12 compares the flux $j(t)$ at four particle

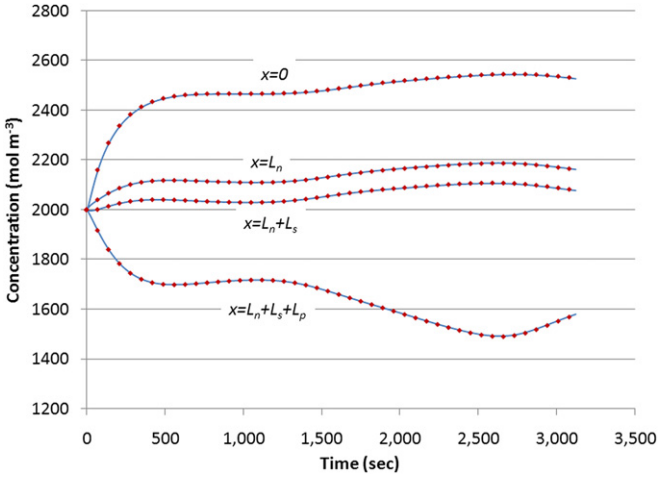

Fig. 11. Concentrations of lithium ion in the liquid phase at the four specified interfaces obtained from the full model (denoted by solid lines) and those from the reduced model (denoted by dotted lines) at 1 C discharge rate.

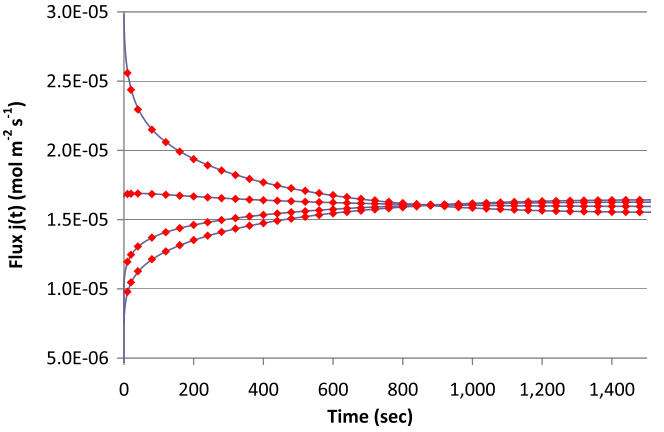

Fig. 12. Surface molar flux $j(t)$ obtained from the full model (denoted by solid lines) and those from the reduced model (denoted by dotted lines) at 1 C discharge rate for a few selected particles.

surfaces, and Fig. 13 compares the surface concentration at the same four particles. Excellent results are achieved by using the reduced model in both Figs. 12 and 13. Note that at the start of the discharging surface concentration and flux change rapidly because of sudden change of current from 0 to 1 C at time of zero. And the reduced model can capture all the transient behavior at the particle surface. In Fig. 14, a charge discharge cycle is simulated for comparison. Again, we observe excellent results from the reduced model.

All of the comparisons performed above show that the reduced model can accurately model the cell behavior and thus can be used to replace the full model. While the full model solves for 100 equations for each particle (except for 200 being used for 10 C discharge), the reduced model solves only 7 equations per particle. Because of that, the reduced model runs much faster. For the cell-cycling simulation shown in Fig. 14, the run-time for the full model is about seven times more than the reduced model.

Note that the reduced model cannot be used to calculate the concentration distribution inside the particles. If such information is valuable, one could use the LTI model for most of the particles except for a few selected ones. For those a few selected particles, full particle diffusion equations are solved and thus concentration distribution is available for those a few particles. This technique does not apply to non-spherical particles though because it is too

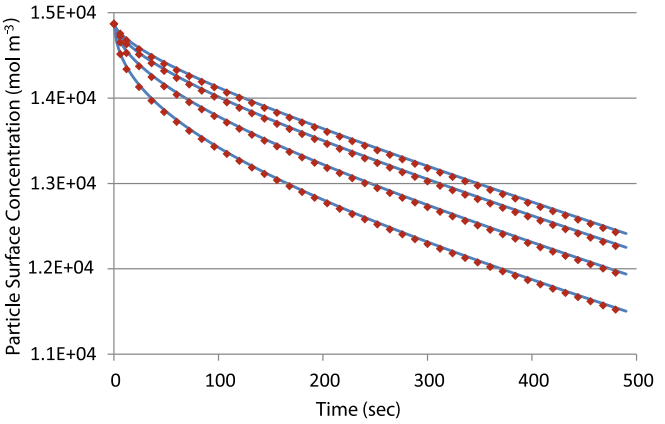

Fig. 13. Surface concentrations obtained from the full model (denoted by solid lines) and those from the reduced model (denoted by dotted lines) at 1 C discharge rate for a few selected particles.

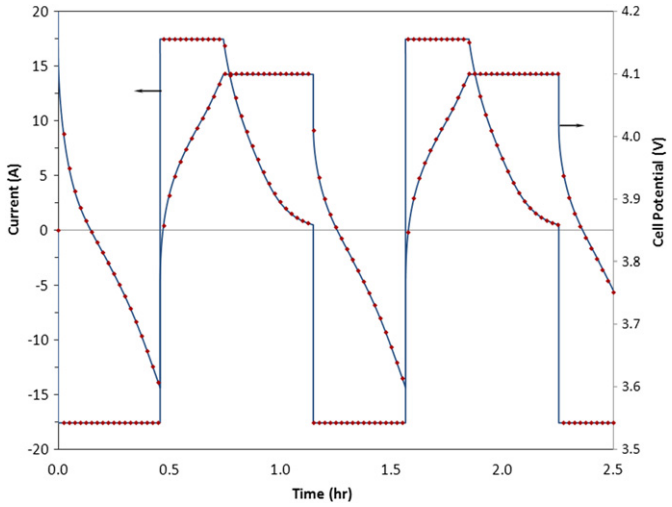

Fig. 14. Cell-cycling simulation results based on the full model (denoted by solid lines) compared to results of the reduced model (denoted by dotted lines). Cell-cycling protocol: 1 C discharge to 3.6 V, followed by 1 C charge to 4.1 V, and then charge the cell holding the cell potential at 4.1 V until the current decreases to 0.5 A.

computationally expensive and too tedious to solve for full 3d diffusion equations even just for one single non-spherical particle in the physics-based cell model. For such non-spherical particles, the LTI approach could provide some additional information without too much additional computational cost. In the LTI models generated so far, we are only interested in averaged surface concentration. We could have, though, added additional outputs when creating the LTI model. For instance, we could have used concentration at a few user specified locations inside the particle as outputs. This would make the LTI model have multiple outputs rather than just one output. With such an LTI model integrated into the physics-based model, concentration at those selected locations can be calculated. One of the nice features about VF is that adding additional outputs does not increase the size of the model linearly. The VF method actually obtained its name because of this feature.

4. Impact of particle shapes on cell performance

In order to investigate the impact of particle shapes on the cell behavior, three models are created, which use spherical particles, elliptical particles, and porous particles, respectively. The properties of these particles are listed in Table 1. The spherical particles have the sizes from Ref. [4]. And the corresponding elliptical particles have the same volume. The porous particles use the same spherical particles with overlapping. For general porous structures, a volume for a porous "particle" is not defined. So, the volume is Table 1 for the porous particle is scaled to be per volume sense, and its surface area is also scaled to reflect that. The increased or decreased specific interfacial area reflects the increased or decreased surface area due to different particle shapes. Apart from the shapes and the specific interfacial area, the rest of the three models are identical. So, any difference in the cell performance is due to the difference in particle shapes. All three models use the LTI approach for the solid diffusion problem.

Table 1
Particle properties. Values for the porous particle are scaled to have the same volume.

	Volume (m^3)	Surface area (m^2)	a_s ($m^2\ m^{-3}$)
Sphere, negative	8.1816e−15	1.96352e−9	$a_{s,n}$
Sphere, positive	2.14464e−15	8.0424e−10	$a_{s,p}$
Ellipse, negative	8.1816e−15	2.10352e−9	1.0713x $a_{s,n}$
Ellipse, positive	2.14464e−15	8.5784e−10	1.0666x $a_{s,p}$
Porous, negative	8.1816e−15	1.73694e−9	0.8846x $a_{s,n}$
Porous, positive	2.14464e−15	7.1143e−10	0.8846x $a_{s,p}$

In Figs 15 and 16, discharge curves are compared for a few different discharge rates. Fig. 15 shows that there is minimum difference using these different particles when the discharge rates are low (<1 C rate). Fig. 16 shows that the cell using the elliptical particles delivers more capacity at these higher discharge rates. This is because the surface area of the elliptical particle is larger and thus concentration gradient inside the elliptical particle is smaller as discussed in Section 2, making it less prone to saturation or depletion. On the other hand, the cell using the porous particle has opposite effect on capacity due to its less surface area. Note that the porous particle here uses the same spherical particles only with overlapping, so the results showed the negative impact of overlapping on cell performances.

5. Conclusion

An LTI model is proposed for the solid-phase diffusion problem in particles used by physics-based lithium-ion cell models. The proposed model has the following advantages compared with commonly used methods:

1. It can be used for non-spherical particles or even porous structures. Loss of accuracy is minimum because the LTI model can give very similar results as one would obtain by solving a 3d diffusion equation.
2. The size of the LTI model is very small. For the test cases simulated, the LTI model needs to solve only 7 equations for each particle, while the full model may need up to 200 equations for each particle if spatial discretization is uniform. So, even for spherical particles, the proposed method can reduce the total size of the problem significantly. Thus, the reduced model runs much faster, a factor of seven observed for the cell-cycling simulation.

The proposed LTI method greatly extends the capability of the physics-based models by allowing for non-spherical particles. And the method also significantly increases the efficiency of such models. Lastly, all are achieved with negligible loss of accuracy.

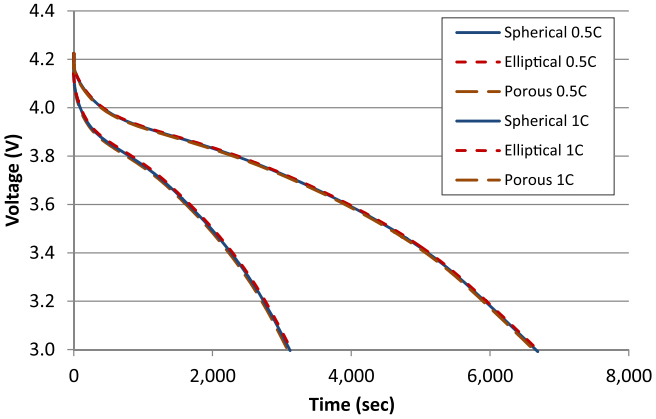

Fig. 15. Cell potential vs. time at different low discharge rates of 0.5 C and 1 C using the three different particle shapes. No apparent differences due to different shapes show up at these low discharge rates.

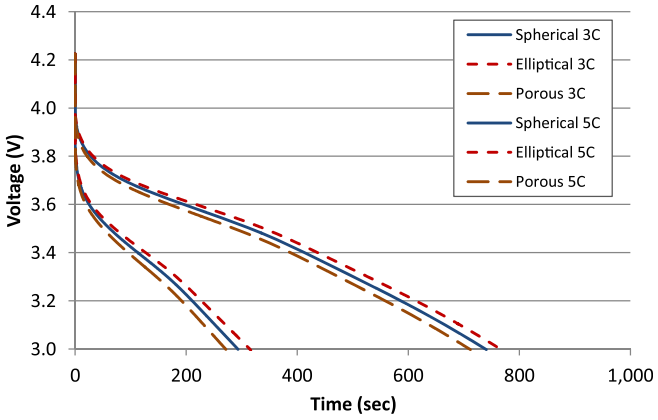

Fig. 16. Cell potential vs. time at different high discharge rates of 3 C and 5 C using three different particle shapes.

List of symbols

a_s	Specific interfacial area, m^{-1}
$a_{s,n}$	Specific interfacial area for negative electrode, m^{-1}
$a_{s,p}$	Specific interfacial area for positive electrode, m^{-1}
c	concentration, mol m^{-3}
c_s	surface concentration, mol m^{-3}
D	diffusivity of lithium in the solid particles, $m^2\ s^{-1}$
j	wall flux of lithium ions, mol $m^{-2}\ s^{-1}$
L_n	thickness of negative electrode, m
L_p	thickness of positive electrode, m
L_s	thickness of separator, m
R	radius of a spherical particle, m
t	time, s
τ	dimensionless time

Appendix A. LTI model identification process for the diffusion problem using vector fitting

In using the VF method for state space model identification, instead of fitting the step response of the state space model to that of the CFD model directly, the transfer function of the state space model is identified with the Fourier transform of the impulse response of the system, which is calculated from the step response. The transfer function of the state space model in Eqn (4) can be shown to be:

$$f(s) = \sum_{i=1}^{N} \frac{c_i}{s - a_i} \tag{A.1}$$

Transfer function is also the Laplace transform of the impulse response of the system. For stable systems, $s = j\omega$ is in the region of convergence of the Laplace transform and thus $f(j\omega)$ becomes the Fourier transform of the impulse response of the state space model. One could then curve-fit $f(j\omega)$ with the sampled Fourier transform of the impulse response, calculated from the step response, to obtain the poles and residuals of Eqn. (A.1). Such a fitting process can be viewed as using rational basis functions $1/(s - a_i)$ for curve-fitting. If a_i were known, this would become a linear least-squares problem to determine c_i. Since a_i are not known, an iterative scheme is needed to update a_i at each iteration. Once the poles and residuals are obtained, it is a simple matter to obtain the corresponding state space model of Eqn (4). The sampled Fourier transform can be obtained by sampling the impulse response of the diffusion problem followed by FFT. Such a fitting approach in the frequency-domain is generally referred to as rational fitting. VF is a robust algorithm of rational fitting [17]. The steps to identify the state space model using VF are summarized as follows:

Step 1 Obtain the step response of the diffusion problem from a CFD model.
Step 2 Calculate the impulse response. The time derivative of the step response is the impulse response.
Step 3 Sample the impulse response curve.
Step 4 Perform FFT of the sampled impulse response.
Step 5 Take the low frequency portion of the FFT and perform proper scaling in both coordinates. This gives the sampled Fourier transform of the impulse response.
Step 6 Perform vector fitting to obtain the poles and residuals of the transfer function of the state space model.
Step 7 Construct the state space model from the known transfer function.
Step 8 Solve the state space model in time-domain.

Some variations of the procedure exist. First of all, one could start with the impulse response if available. For the diffusion problem, it is easier for a CFD solver to calculate the step response than the impulse response. Secondly, if the solver has the frequency sweep capability, the sampled Fourier transform can be obtained directly and this could then be the starting point. The above procedure assumes that the Fourier transform of the impulse response exists. For the solid-phase diffusion problem, the impulse response has no Fourier transfer. This is because the surface concentration approaches to a positive steady state value as time goes to infinity under an impulse flux boundary condition. Such a behavior is simply a consequence of mass conservation. In order to apply the above procedure, a small modification is necessary, which is to apply the above procedure *after* the steady state value is subtracted from its impulse response. And then an integrator is added in the final transfer function to account for the steady state value. Fig. A1 shows the numerically calculated impulse response (not a unit impulse response) for the particle used in the negative electrode. The corresponding step response has a step input of 1e−6 mol $m^{-2}\ s^{-1}$ *into* the sphere rather than a unit step input. Since the system is linear, a proper scaling will give the *unit* impulse response. Fig. A2 shows the numerically calculated frequency response by performing FFT of the impulse response followed by proper scaling. Only first 1200 points from FFT is used for fitting and displayed in Fig. A2. Experience suggests that accurate results in time-domain can be obtained when a cut-off frequency is chosen such that the magnitude of the frequency response drops by 1.5–2 orders of magnitude.

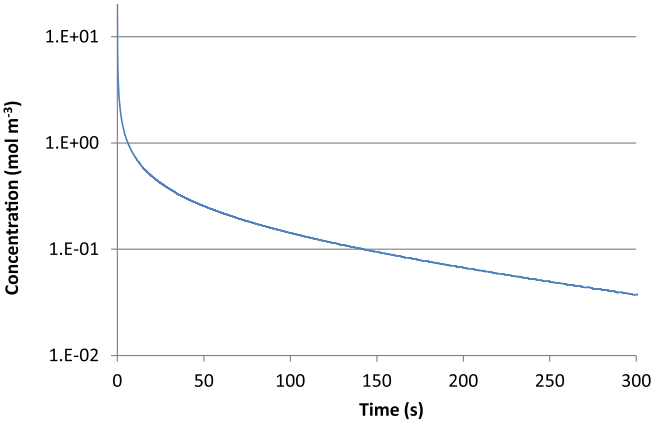

Fig. A1. Impulse response for the spherical particle for the negative electrode.

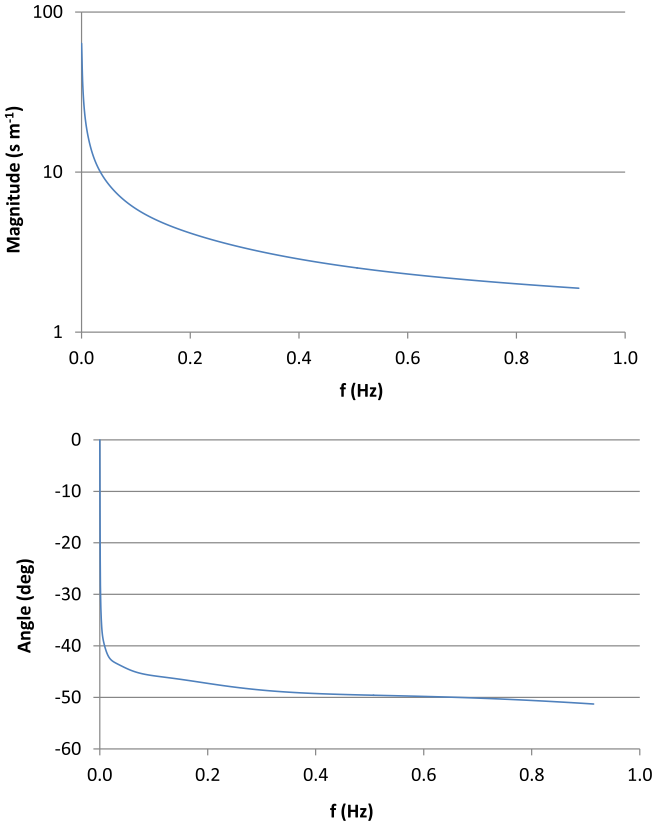

Fig. A2. Numerically calculated frequency response from FFT of the impulse response.

Appendix B. Vector fitting results for spherical particles using analytical solution

For spherical particles, the LTI model could be identified using analytical step response solution rather than CFD solution. Such an analytical solution in non-dimensional form is shown in Ref. [8] to be an infinite series,

$$c_s(\tau) = 3\tau + \sum_{n=1}^{\infty} Q_n(\tau) \tag{B.1}$$

where

$$Q_n(\tau) = \frac{2}{\lambda_n^2}\left[1 - \exp\left(-\lambda_n^2\tau\right)\right] \tag{B.2}$$

$$\lambda_n - \tan(\lambda_n) = 0 \quad n = 1, 2, \ldots \tag{B.3}$$

$$\tau = \frac{D}{R^2}t \tag{B.4}$$

The first 500 terms of the series is used here to represent the analytical solution. Fig. B1 below shows the step responses from the analytical solution and the LTI model. It can be seen that very accurate results are obtained using the LTI model. Below is the state space model from the VF method used to generate the two plots in Fig. B1. Such a state space model can be integrated into the physics-based cell model for the diffusion problem using spherical particles after scaling back to dimensional form. Note that matrix A in the state space model takes diagonal form, which makes the 7 equations in the state space model decoupled. Such a simple form makes the already small model very efficient to solve.

Initial conditions: $x_0 = 0.0$; $x_1 = 0.0$; $x_2 = 0.0$; $x_3 = 0.0$; $x_4 = 0.0$; $x_5 = 0.0$; $x_6 = 0.0$;

c_surf = 366.4550 * x_0 + 38.89143 * x_1 + 16.43058 * x_2 + 7.834168 * x_3 + 3.825026 * x_4 + 2.198156 * x_5 + 3.0 * x_6;

$dx_0/dt = -6.084373e + 004 * x_0 + flux\_j$;

$dx_1/dt = -5.807664e + 003 * x_1 + flux\_j$;

$dx_2/dt = -1.307607e + 003 * x_2 + flux\_j$;

$dx_3/dt = -3.227365e + 002 * x_3 + flux\_j$;

$dx_4/dt = -8.353250e + 001 * x_4 + flux\_j$;

$dx_5/dt = -2.089056e + 001 * x_5 + flux\_j$;

$dx_6/dt = flux\_j$;

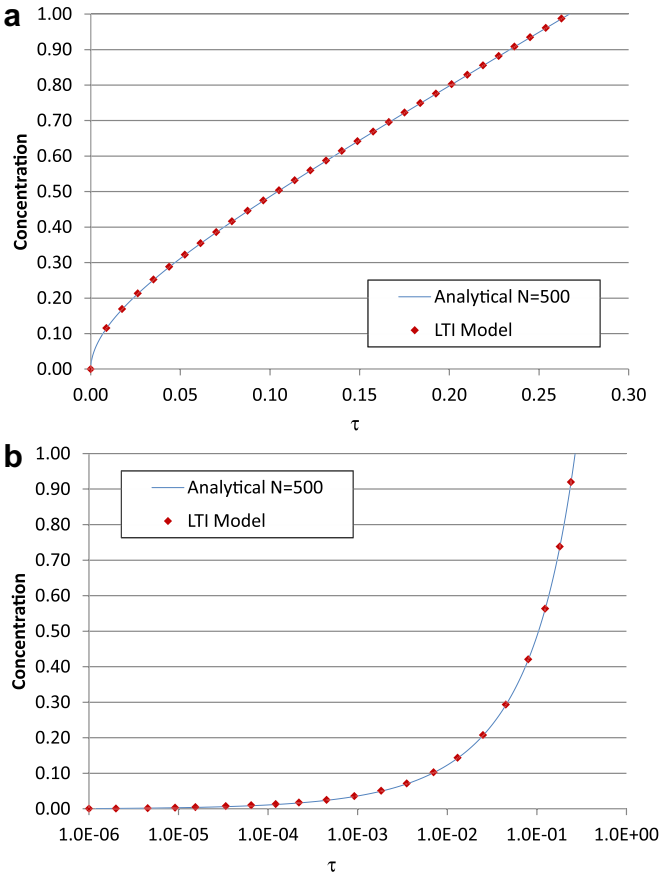

Fig. B1. Step responses in non-dimensional form from the analytical solution and the LTI model for a spherical particle. a) Regular scale on τ. b) Log scale on τ.

References

[1] M. Doyle, T.F. Fuller, J. Newman, J. Electrochem. Soc. 140 (6) (1993) 1526–1533.
[2] T.F. Fuller, M. Doyle, J. Newman, J. Electrochem. Soc. 141 (1) (1994) 1–10.
[3] M. Doyle, J. Newman, J. Electrochem. Soc. 143 (6) (1996) 1890–1903.
[4] L. Cai, R.E. White, J. Electrochem. Soc. 156 (3) (2009) A154–A161.
[5] K.A. Smith, C.D. Rahn, C.-Y. Wang, Energy Convers. Manage. 48 (2007) 2565–2578.
[6] C.Y. Wang, W.B. Gu, B.Y. Liaw, J. Electrochem. Soc. 145 (10) (1998) 3407–3417.
[7] V.R. Subramanian, D. Tapriyal, R.E. White, Electrochem. Solid-State Lett. 7 (9) (2004) A259–A263.
[8] M. Guo, R.E. White, J. Power Sources 198 (2012) 322–328.
[9] K.A. Smith, C.D. Rahn, C.Y. Wang, J. Dyn. Syst. Meas. Control 130 (2008) 011012 1–8.
[10] J.L. Lee, A. Chemistruck, G.L. Plett, J. Power Sources 206 (2012) 367–377.

[11] A. Morched, B. Gustavsen, M. Tartibi, IEEE Trans. Power Del. 14 (3) (1999) 1032–1038.
[12] B. Gustavsen, IEEE Trans. Power Del. 19 (1) (2004) 414–422.
[13] E.P. Li, E.X. Liu, L.W. Li, M.S. Leong, IEEE Trans. Adv. Packag. 27 (1) (2004) 213–223.
[14] G. Antonini, IEEE Trans. Electromagn. Compat. 45 (3) (2003) 502–512.
[15] X. Hu, S. Lin, S. Stanton, W. Lian, IEEE Trans. Ind. Appl. 47 (4) (2011) 1692–1699.
[16] X. Hu, L. Chaudhari, S. Lin, S. Stanton, S. Asgari, W. Lian, IEEE ITEC Conf. Dearborn. (2012) IT-0065.
[17] B. Gustavsen, A. Semlyen, IEEE Trans. Power Del. 14 (3) (1999) 1052–1061.
[18] X. Hu, S. Stanton, SAE paper 2012-01-0665.